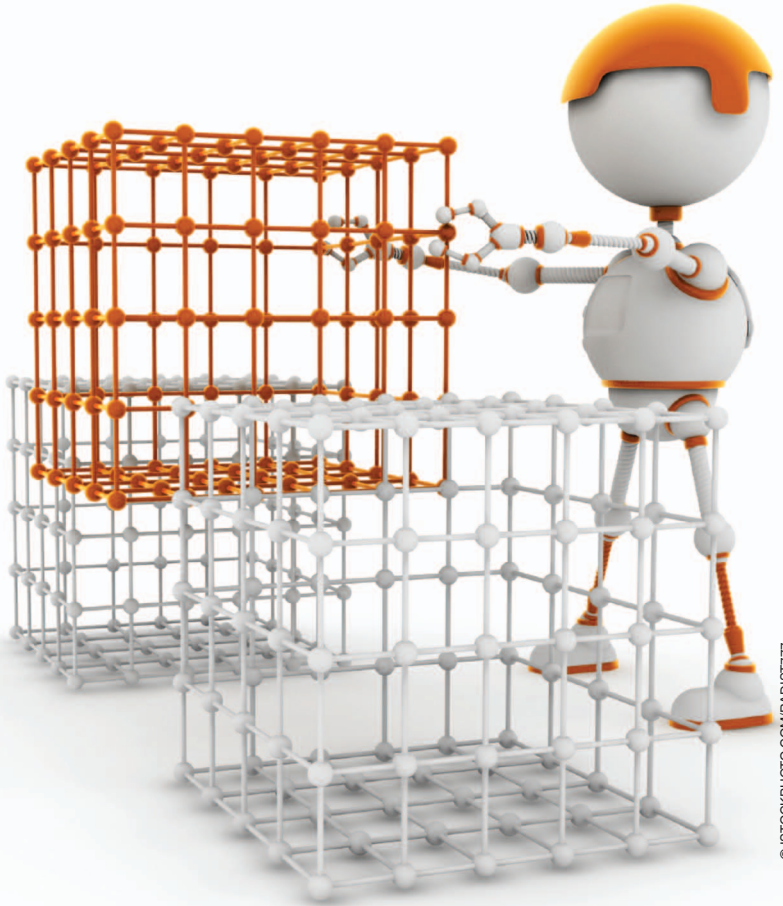


By Franz Nigl, Shuguang Li,
Jeremy E. Blum, and Hod Lipson

Autonomous Truss Reconfiguration and Manipulation



©ISTOCKPHOTO.COM/RADIST777

Structure-Reconfiguring Robots

In this article, we present a robot capable of autonomously traversing and manipulating a three-dimensional (3-D) truss structure. The robot can approach and traverse multiple structural joints using a combination of translational and rotational motions. A key factor in allowing reliable motion and engagement is the use of specially designed structural building blocks comprised of bidirectional geared rods. A set of traversal plans, each comprised of basic motion primitives, were analyzed for speed, robustness, and repeatability. Paths covering eight joints are demonstrated, as well as automatic element assembly and disassembly. We suggest that the robot architecture and truss module design, such as the one presented here, could open the door to robotically assembled,

maintained, and reconfigured structures that would ordinarily be difficult, risky, or time consuming for humans to construct.

Design of Robot

Structure-climbing robots have traditionally been developed to perform tasks currently carried out by humans, which range from structural inspections to cleaning and maintenance. Our goal in this article is to explore both robot and structure design to expand the range of tasks which can be successfully completed autonomously. Specifically, we are interested in the design of a robot capable of modifying a structure by taking it apart and rebuilding it into a different shapes. Such structure-reconfiguring robots could have a profound impact on construction processes, especially activities involving frame construction. In the longer term, the ability to autonomously

Digital Object Identifier 10.1109/MRA.2012.2201579

Date of publication: 21 June 2013

Table 1. Summary of climbing robots.

Author (Robot)	Connecting Mechanism (Structure Type)	Description and Purpose
Aracil et al., 2006 [5]	Mechanical gripper	Parallel-climbing robot based on Stewart–Gough's platform for climbing on palm trees and within complex structures.
Balaguer et al., 2002 (Roma 1) [6]	Mechanical gripper	Large, untethered inspection robot for structures. Robot mass is 70 kg.
Balaguer et al., 2002 (Roma 2) [6]	Suction cups (smooth surfaces)	Inspection robot for moving within structures.
Chatzakos et al., 2006 [7]	Mechanical pipe-clamping mechanism	Tethered, omnidirectional pipe inspection robot capable of traversing pipe bends and branches.
Chen and Yeo, 2003 [8]	Suction cups	Tethered walking robot capable of traversing on flat surfaces.
Daltonio et al., 2009 [9]	Mechanical and adhesive mechanism	Small robot that demonstrates climbing with different mechanic and adhesive connection mechanisms that include hooks, spines, adhesive tapes, and Velcro.
Elliot et al., 2007 (City-Climber) [10]	Suction mechanism	Untethered wall-climbing robot.
Fu et al., 2008 [11]	Suction mechanism	Wheel-leg hybrid robot capable of moving on horizontal and vertical surfaces.
Goldman, 2009 (HyDRAS) [12]	Robot clamps around structure.	Snake like climbing robot.
Hillenbrand et al., 2008 (Cromsci) [13]	Suction mechanism	Inspection robot for concrete walls.
Hjelle, 2009 [27]	Bidirectional gearing system	Three-dimensional (3-D) truss construction robot.
Kalra et al., 2006 [14]	Permanent magnet mechanism	Oil tank inspection robot.
Kennedy et al., 2006 (Lemur IIb) [15]	Mechanical gripping/holding mechanism	Free-climbing robot.
Kotay and Rus, 1996 [16]	Magnetic mechanism	Tethered inchworm robot for climbing on 3-D structures.
Krosuri and Minor, 2005 [17]	Suction or magnetic mechanism	Tethered biped robot for climbing and walking using a hybrid hip joint.
Minor and Mukherjee, 2003 [18]	Suction cups	Small, tethered biped robot.
Sattar et al., 2009 [19]	Mechanical mechanism	Ring-climbing robot for inspection of wind turbines. Ring-type robot is assembled around wind turbine pole.
Skaff et al., 2001 (Skyworker) [1]	Mechanical gripper	Climbing robot with the ability to add and remove individual beams under simulated zero gravity.
Spenko et al., 2008 (RiSE) [20]	Interlocking and bonding mechanism	Biologically inspired hexapod untethered robot that uses locking and bonding mechanism to climb walls and trees.
Sun et al., 2004 [21]	Suction cups (glass surface)	Cleaning robot for glass walls of high-rise buildings.
Tâche et al., 2009 (MagneBike) [22]	Magnetic mechanism (ferrous pipes)	Two-wheel bike like tethered robot for inspection of large ferromagnetic pipes with complex-shaped geometries.
Tavakoli et al., 2005 [23]	Mechanical gripper	Parallel/serial hybrid pole-climbing robot.
Tavakoli et al., 2008 (3-DCLIMBER) [24]	Mechanical gripper	Tethered climbing robot for inspection of 3-D structures.
Terada et al., 2008 [29] (AMAS) [29]	Mechanical gripper	Robot that can build and climb on a structure created of passive cube elements.
White et al., 2005 [25]	Suction mechanism	Tethered manufacturing and inspection robot.
Yun et al., 2008 (Shady3-D) [2]	Mechanical gripper	Structure-climbing robot. Three motive degree of freedom (DoF) robot that can combine with a second robot to create a six-DoF robot.

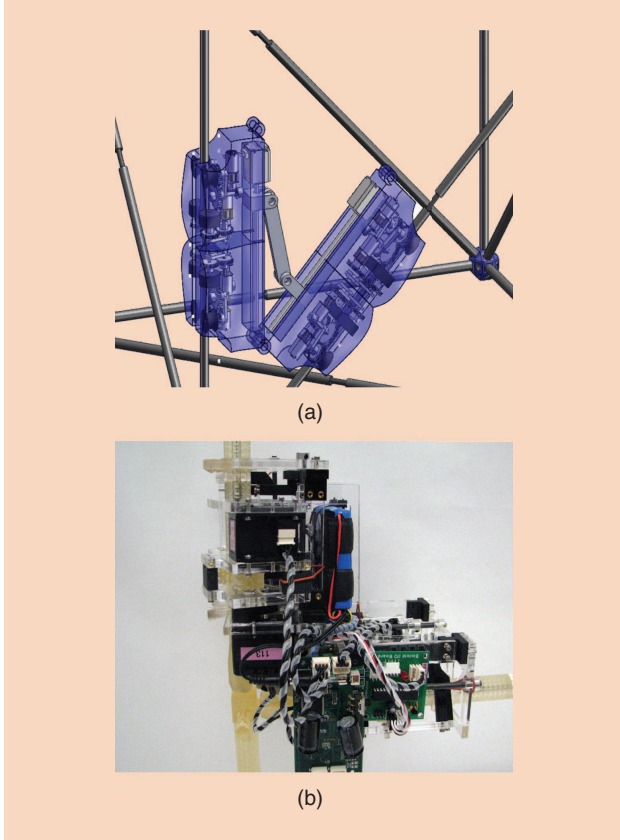


Figure 1. Truss-reconfiguring robot: (a) concept and (b) implementation.

repair a damaged structure or autonomously adapt an existing structure to a new function can have applications ranging from disaster recovery to space exploration.

One of the key challenges in designing a structure-reconfiguring robot is that most current structural building blocks are designed for manipulation by humans, not by machines. Structural joints require complex assembly, and truss

elements are cumbersome to manipulate. The development of standards for joint connections and elements has been crucial in the progress of modular assembly in the construction industry. Furthermore, the lack of robot-friendly joints and elements has significantly limited the deployment of robots in the construction field.

We explore the codesign of both a robot and structural components for the explicit purpose of robotic structure reconfiguration. Two different robots are described. Robot version one (R1) is used to demonstrate motion within a test structure. By executing a series of climbing motions, R1 can maneuver between the horizontal and vertical planes of a structure and traverse multiple nodes in one run. The second version of the robot (R2) is capable of demonstrating disassembly of an entire vertical structural plane and assembly of individual truss components. The two robots represent two generations of development in our project. A picture of the concept as well as robot R2 during disassembly can be seen in Figure 1.

Background and Previous Work

Numerous designs exist that demonstrate robots climbing on walls, traversing poles, and navigating truss-like or tubular structures. Only a few present the ability to manipulate these structures or demonstrate performance statistics about traversing multiple joints—a key performance metric.

An overview of the different climbing robots is provided in Table 1. Attachment mechanisms used include suction cups, magnetic mechanisms, gripping mechanisms, and adhesive mechanisms. From this group, only Skywalker [1] demonstrated the ability to add a beam to a structure. Shady 3-D [2], [26], [28] demonstrated the ability to create a higher degrees of freedom (DoF) robot using two Shady 3-D robots connected with a passive module. Several structural designs were simulated that could be built with passive elements and Shady 3-D robots. Dogget [3] designed a

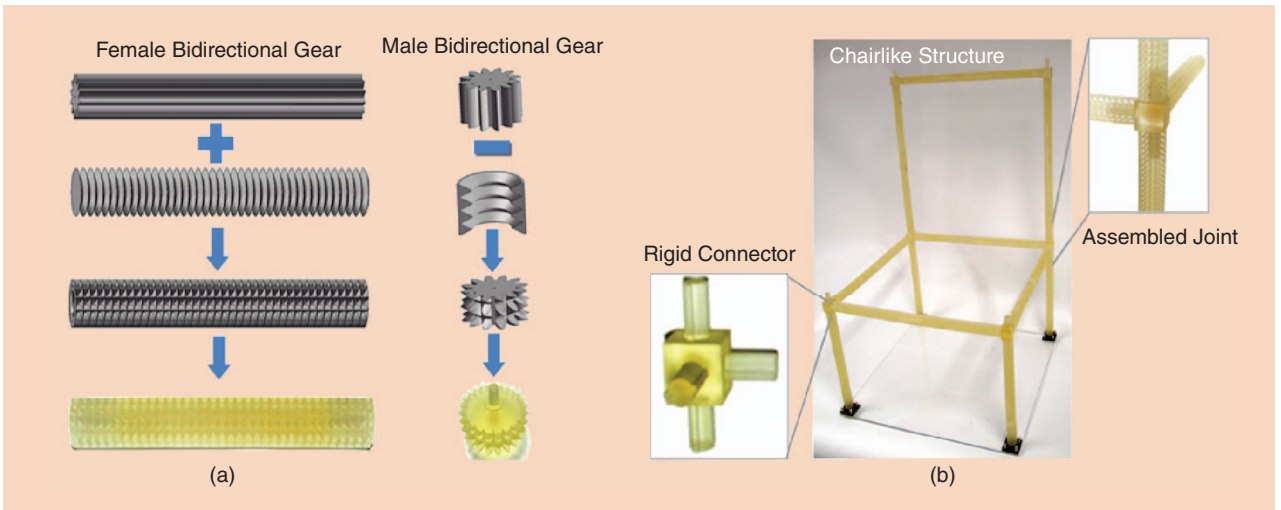


Figure 2. Truss structure: (a) design of bidirectional gear rod and (b) fully assembled chairlike structure using rigid connectors.

robot capable of building a 3-D structure composed of 102 truss elements, but the robot is stationary and cannot climb to any point in the structure for inspection or repair. Galloway et al. [4] built a similar system that can create 3-D structures layer by layer using a robot fixed to the floor. Automatic modular assembly system (AMAS) [29] includes an assembler robot and passive cube-shaped building blocks. It showed the automatic construction capability for 3-D structures. The robot presented in this article is a further development of a design shown by Hjelle [27]. This robot exhibited two identical halves connected via a hinge joint. Each side had a translational and a rotational mechanism, similar to the robot presented in this article. The robot did not exhibit any feedback and was open-loop controlled. The robot engaged onto a 1/8-in pinion wire with 16 threads per inch. Testing of the original design showed the need for improvements of the hardware and electronics. The pinion wire gearing/threading was not adequate and needed bigger teeth to allow better engagement by the robot mechanism. Additionally, it was determined that position feedback from the motors would be required if significantly improved control was to be achieved. All of these issues are addressed and resolved using the robots demonstrated in this article.

Structural Truss Design

The structural components have to fulfill three primary criteria to ensure a reliable interaction with the robot. First, the parts have to be strong enough to support the robot but light enough to be handled by the robot. Second, the robot has to lock and unlock the connectors, so the entire structure may be reconfigured. Lastly, the robot has to reliably engage, rotate, and translate on an individual rod.

Initial designs utilized cylindrical rods which the robot engaged via rubber wheels. Using this method of attachment, translation and rotation of the robot along and around the rod resulted in slippage. To avoid the problem of slippage and to increase the power transmitted from the robot to the rod, bidirectional gearing was developed for the rods and the robot [Figure 2(a)].

Rod Design

These novel bidirectional geared rods have gearing in the longitudinal direction as well as in the rotational direction, allowing for increased power transmission from the robot to the rod regardless of the plane of travel. Uniquely, these bidirectional gears allow motion in one direction while inhibiting motion in the orthogonal direction, thus arresting slippage. This enables the robot to remain at the unstable position on top of the rod while successfully translating along the rod.

The bidirectional gearing system consists of a pair of gears: a female bidirectional gear and a male bidirectional gear. The female bidirectional gearing is used on the rods, whereas the robot uses the male bidirectional gearing with its servos to effectively engage the structure.

To create the female bidirectional gears, a contour of a spur gear rack was revolved around a rod axis and was merged with a spur gear thread in the orthogonal direction. The different design stages of the female bidirectionally geared rod can be seen in Figure 2(a). To create the male bidirectional gear, the outside contour of a spur gear rack was revolved around and subtracted from a spur gear. Figure 2(a) shows the CAD drawings of the steps on sample gears and pictures of the 3-D printed actual bidirectional gears.

Connector Design

To join the rods together at their vertices, two different types of connectors were designed: a fixed connector and a robot-lockable connector. A fixed connector, for traversal by robot R1, was designed to securely connect structural elements together, which could not be manipulated by the robot. In this structural iteration, the angles between the rods are nearly orthogonal, which required less flexibility from the robot to

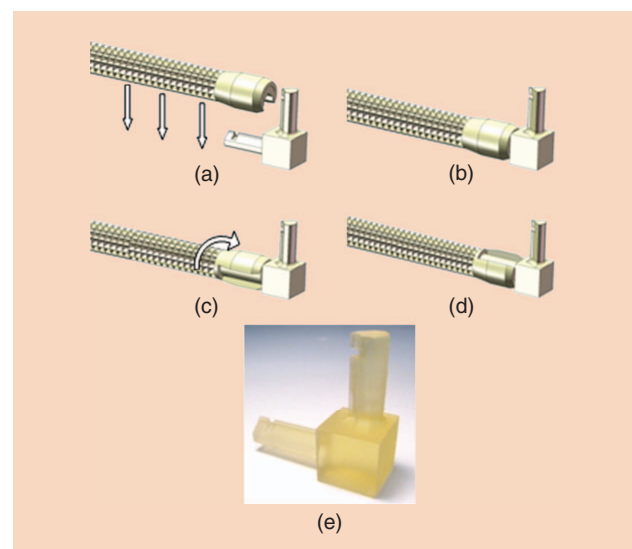


Figure 3. Assembly of connector: (a) rod approaching connector, (b) rod in unlocked state on connector, (c) rod twisting into locking position, (d) rod in locked position, and (e) photo of 3-D printed connector node.

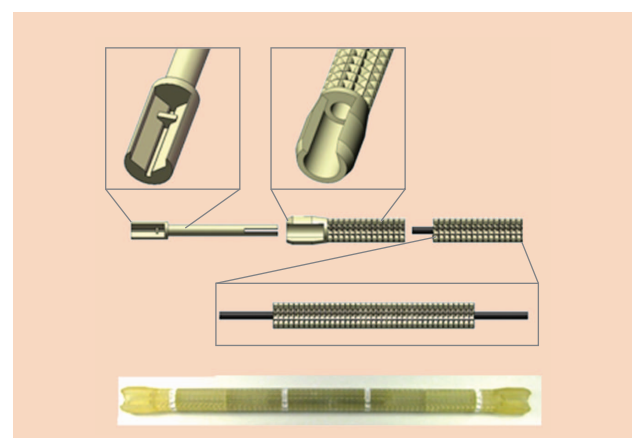


Figure 4. Rod with female part of lockable connector.

Table 2. Comparison of two robots.

Parameter (Component)	Robot R1	Robot R2
Height	89 mm	119 mm
Length	318 mm	318 mm
Width	178 mm	190 mm
Mass	1633 g	1740 g
Translational cam servo (x2)	AX-12+	AX-12+
Translational servo (x2)	AX-12+	AX-12+
Rotational cam servo (x2)	AX-12+	AX-12+
Rotational servo (x2)	AX-12+	RX-28
Hinge servo (x1)	AX-12+	RX-28
Controller	CM-5	CM-2+
Battery location	On side of robot	At bottom of robot
Programming	Graphical	C-Code
Position feedback	Rotational angle of servos	Rotational angle of servos, reflectivity sensor feedback

compensate for non-90° angles, and resulted in a greater chance of success when traversing over nodes. In the second design iteration, the connectors were modified to allow them to be locked and unlocked by robot R2. These robot-configurable joints were needed to allow the robot to independently reconfigure the structure. However, they resulted in more flexible connection points at the nodes of the truss structure, which necessitated a robot with better compensation for non-orthogonal joints between rods. Also, the current design allows the robot to open and close the connectors from only one direction and hence disassemble or assemble a rod from a specific side only.

1) *Rigid Connectors—Iteration 1 (Robot Traversal Only)*: In the rigid connection scheme, individual rods are connected to the center nodes by simple extensions. The rigid connec-

tors can be seen in Figure 2(b). Truss elements were printed in pieces, as an entire truss could not be printed because of the size restrictions of the 3-D printer. A node with four rods connected to it can be seen in Figure 2(b).

2) *Lockable Connectors—Iteration 2 (Robot Manipulation)*: Robot R2 was designed with the intention that it would reassemble a truss structure; connectors were redesigned to enable this action. The lockable connectors can be locked and unlocked by the robot and hence they allow the disconnection and removal of individual trusses from the structure. The lockable connectors consist of a male connector part on the node (Figure 3) and a female part on the truss element (Figure 4). These connectors are closed or opened by turning the cylindrical locking element 180°, as illustrated in Figure 3. The rods themselves were stiffened using a carbon fiber rod as can be seen in Figure 4.

Robot Design

Two different versions of the robot were built. Robot iteration 1 (R1) was designed to demonstrate traversal in the fixed connector structure. As lockable connectors were introduced in the structural design, deficiencies observed with R1 required a design upgrade to robot iteration 2 (R2). This robot has stronger servos, uses sensors, and includes an upgraded controller and software.

For both robots, the body consists of 3- and 6-mm-thick laser-cut acrylic, rapid-prototyped plastic printed by a Stratasys Dimension 3-D printer, and gears printed by an Objet Eden 260 V 3-D printer. Nine servos on each robot, controlled by an Atmel-based microcontroller board and accompanying software, provide the actuation. Both versions of the robot use servo and control units from Robotis Inc.

Traversal Robot—Iteration 1 (R1)

R1 consists of two mechanically identical halves connected via a hinge. Each side is comprised of a translational and a rotational mechanism and utilizes a total of four actuators. The translational mechanism carries out the longitudinal robot movements along the rod, whereas the rotational mechanism drives angular motions around the rod. R1 was built to demonstrate traversal in a 3-D structure. Its main dimensions can be seen in Table 2.

A single actuator is used to provide hinge motion between the two identical robot halves. It is directly connected to each side without any gearing.

The translational mechanism on each side consists of two servo actuators. One servo utilizes a cam to engage the translational system, and the other servo propels the robot along the rod using a 12-tooth bidirectional male gear engaged on the rod.

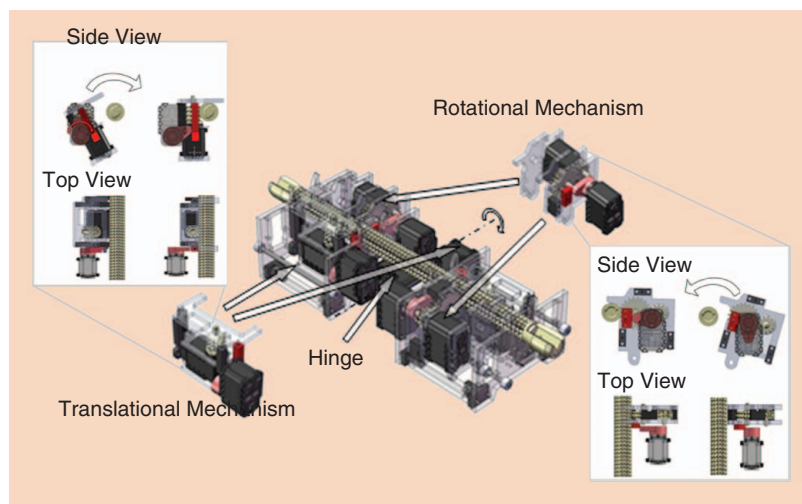


Figure 5. Robot motion mechanisms.

The self-locking engagement system is powered down following successful engagement to preserve battery power. The translational mechanism is displayed in Figure 5.

Similar to the translational system, the rotational mechanism uses an actuated cam to engage the rotational motor. The cam servo locks automatically and is powered down when the rotational assembly has been engaged successfully. In contrast to the translational mechanism, the rotational actuator gear is not directly engaged with the rod, because it is not sufficiently large enough to transfer the necessary amount of torque needed for the robot to perform all required motions. Therefore, a 12:22 gear ratio is utilized to increase the torque delivered to the rod. The rotational mechanism is displayed in Figure 5. It is comprised of a 12-tooth female bidirectional gear and a 22-tooth male bidirectional gear. The female gear is connected to the output shaft of the actuator and the male gear is designed to engage with the structure.

R1 exclusively uses AX-12+ (1.2-Nm torque) servos in combination with a CM-5 control module. No feedback through external sensors is used for this robot. The servos communicate with the control module via a TTL signal and can be dynamically changed between continuous rotational mode and angular servo mode. Limits for torque, speed, angular position, and temperature values are all stored in onboard memory in each servo; these values can be set or read by the program running on the control module. Power for the system is provided entirely by a 12-V rechargeable lithium ion battery, allowing for untethered operation.

Robot version R1 was programmed using the *Behavior Control Program* graphical programming language. The program was compiled into a hex file and downloaded onto the control module where it was executed. Control of R1 is achieved entirely by setting motors to prescribed angular rotations in the program.

Manipulation Robot—Iteration 2 (R2)

Robot R2 is an improved version of R1 that is capable of manipulating the lockable connectors and can therefore perform more complex assembly and disassembly actions. Imbalance caused by the battery, weak servos, and simplistic programming make manipulating the lockable connectors using R1 highly unreliable. These problems were addressed and resolved in R2.

The translational motion is the same as in robot R1. The design proved satisfactory for the translation of the robot in the structure and hence no changes had to be made.

Tests with R1 showed that the servos for the rotational mechanism needed to be upgraded to improve reliability of the 180° rotation motion. The rotational motors were switched out in favor of RX-28 (2.7-Nm torque) servos, which use the RS485 communication protocol in contrast to the half-duplex asynchronous serial communication used with the AX-12+ servos.

Preliminary disassembly tests showed that the hinge servo in robot version R1 needed to be replaced with a stronger

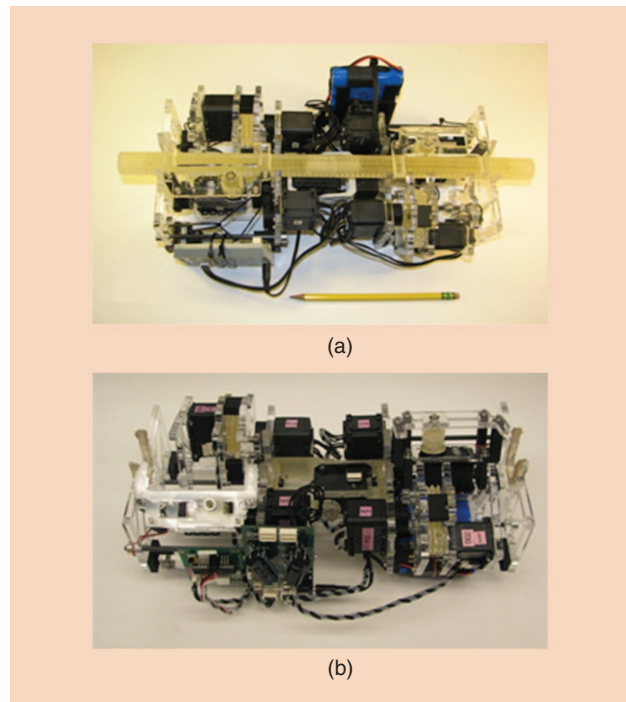


Figure 6. Two versions of the robot: (a) Robot R1 and (b) Robot R2.

motor to ensure that the robot could properly and reliably react to deviations in the orthogonal angle that was expected at joints. Therefore the hinge servo was replaced with a RX-28 servo as well.

Unlike in R1, the 12-V battery was mounted to the underside of the robot [Figure 6(b)] to effectively eliminate the weight distribution problem faced by R1.

Upgrading the CM-5 to the CM-2+ controller was necessary both to communicate on the RS485 bus used by the stronger servos and to communicate with external sensors. R2 was outfitted with two Fairchild Semiconductor QRD1114 reflective object sensors and accompanying circuitry to send analog sensor information to the controller via an intermediary I/O board. By detecting white acrylic paint markings on the rods (Figure 4) using these sensors, it was possible for the robot to determine its relative position and to proceed accordingly. Software filtering and an adjustable hardware mounting bracket allow these sensors to be calibrated as needed.

Robot R2's microcontroller was programmed entirely using the C language. This resulted in a far more advanced control scheme, and the ability to react based on sensor inputs. Isolated motions were preprogrammed (i.e., advancing forward, releasing a truss, etc.), but the timing of these actions was determined by filtered information from the reflectivity sensors. Consequently, R2 could exhibit autonomous translational movement, whereas R1 could not.

Traversal Motions (Robot R1)

To achieve relocation within the structure, the robot needed to perform a series of basic motions. We identified three basic motions that needed to be performed by the robot to

Table 3. Basic motions of Robot R1.

Basic Motions	Steps
Translational motion	<ol style="list-style-type: none"> 1) Disengage one translational mechanism. 2) Decrease the hinge angle. 3) Activate second translational mechanism and move robot to the center of the rod. 4) Operate the hinge to align the second translational mechanism to the rod and engage it.
90° vertical rotation	<ol style="list-style-type: none"> 1) Disengage the translational mechanism on the horizontal rod. 2) Reduce the hinge angle slightly. 3) Move robot on vertical rod away from node. 4) Engage the rotational mechanism on the vertical rod, disengage the translational mechanism and rotate the robot 90° in the desired direction. 5) Engage the translational mechanism on the vertical rod and disengage the rotational mechanism. Move the robot to the horizontal rod. 6) Move the hinge so that the two robot halves are perpendicular. Engage the translational mechanism on the horizontal rod.
180° horizontal rotation	<ol style="list-style-type: none"> 1) Engage the rotational mechanism and disengage the translational mechanism on each robot half. 2) Rotate the robot 180° by using both rotational mechanisms. 3) Engage the translational mechanism and disengage the rotational mechanism on each robot half.

reach any point in a cubed truss structure. We used a chair-like test bed, as this structure exhibits a vertical and horizontal plane. This permitted us to demonstrate traversal in both planes, as well as transitions between the planes.

Basic Motions

Three basic motions were identified, which in conjunction with one another, allow the robot to reach any point within the structure: translational motion, 90° vertical rotation, and 180° horizontal rotation.

1) *Translational Motion:* To advance in a 3-D structure, the robot has to be capable of moving along a truss. The robot's starting position has both robot halves connected to rods with the translational mechanism engaged. The robot shown in Table 3 starts attached to the bottom of a horizontal rod. The robot could also be attached to the top of the horizontal rod as an alternative starting point (the path would be the same, but inverted). The robot then performs the steps as shown and described in Table 3.

This leaves the robot in a position having both translational mechanisms engaged at the center of the rod. The same steps would be performed, but in reverse order, to advance to the other end of the rod. The same motion and steps can be performed on a vertical rod with the robot moving either up or down.

2) *90° Vertical Rotation:* This motion lets the robot move between rods in the horizontal plane with the aid of a vertical rod. The initial position is the same as for the translation motion. Both translation mechanisms are engaged on two perpendicular rods. As shown in Table 3, the robot is located at the bottom of the horizontal rod. The robot could also start out by being attached above the horizontal rod. The robot then performs the steps as shown and described in Table 3.

3) *180° Horizontal Rotation:* This motion lets the robot move from the underside of a horizontal rod to the top and vice versa. The starting position engages both rotational mechanisms of the robot on the middle of a rod. The robot could either be above or below the horizontal rod. When starting below the rod, the robot performs the steps as shown and described in Table 3.

This results in a final position that is nearly identical to the starting point for the translational motion. The slight difference is that only one translational mechanism is engaged. Therefore, when continuing with the translational motion, the command to release the translation mechanism will not be executed.

Test Bed

To test the robot motion within the structure and to evaluate the robot's performance with respect to the different basic

motions, R1 was programmed to navigate throughout a chair-like structure.

This structure comprises a vertical and a horizontal square plane, which is the minimal needed test bed for the robot. Any bigger sized structure would just consist of additional vertical and horizontal planes. This structure also allows for the testing of the robot's transition between the two planes. The steps performed by the robot can be seen in Figure 7 and are described below.

- Step 1) Start out on the front, lower side of the horizontal rod and travel to the right.
- Step 2) Move to the right lower horizontal rod and travel to the end of the right lower horizontal rod.

- Step 3) Move to the lower back rod.
- Step 4) Rotate to the top of the lower back rod.
- Step 5) Move to the vertical left rod.
- Step 6) Connect to the left vertical rod and move upwards to the horizontal top rod.
- Step 7) Traverse at the bottom of the top vertical rod.
- Step 8) Move down the right vertical rod.
- Step 9) Move to the top side of the back horizontal rod.
- Step 10) Rotate to the bottom side of the back horizontal rod.
- Step 11) Move to the left side of the back horizontal rod.
- Step 12) Move to the left lower rod before moving to the front lower bar (the original position).

Table 4. Basic motions of Robot R2.

Basic Motions	Steps
Translational motion	<ol style="list-style-type: none"> 1) Disengage one translational mechanism. 2) Activate second translational mechanism and move the robot until the reflectivity sensors detect the stop marking. 3) Operate the hinge to align the second translational mechanism to the rod and engage its translational mechanism.
Disassembly motion	<ol style="list-style-type: none"> 1) Open the hinge slightly and engage the second translational mechanism, adjust the hinge angle to 90°. (This step is critical for ensuring that there is no discrepancy between the angle of the male and female gearings.) 2) Disengage the translational mechanism halfway (so as to hold the rod in place without preventing it from rotating) and engage the rotational mechanism. 3) Disengage the translational mechanism completely and operate the rotational mechanism for 180°, unlocking the connector. Disengage the rotational mechanism to release the rod.
Vertical assembly motion	<ol style="list-style-type: none"> 1) Align rod with connector. 2) Operate the rotational mechanism for 180° to lock the connector. Disengage the rotational mechanism and engage the translational mechanism. (If the rotational mechanism was not turned 180°, the engagement of the translational mechanism will correct misalignments up to 15°.)
Disassembly, 90° rotation, and reassembly of truss	<ol style="list-style-type: none"> 1) Perform disassembly motion (1)–(3) as described above on horizontal rod without performing the last step of releasing the rod. 2) Decrease hinge angle slightly and move robot away from node. 3) Engage rotational mechanism on vertical rod and disengage translational mechanism. 4) Rotate robot 90°. 5) Engage translational mechanism on vertical rod and disengage rotational mechanism. 6) Set hinge angle to 90° and translate robot to node using feedback from reflectivity sensors. 7) Operate the rotational mechanism for 180°, locking the connector. Disengage the rotational mechanism and engage the translational mechanism. (If the rotational mechanism was not turned 180°, the engagement of the translational mechanism will correct misalignments up to 15°.)

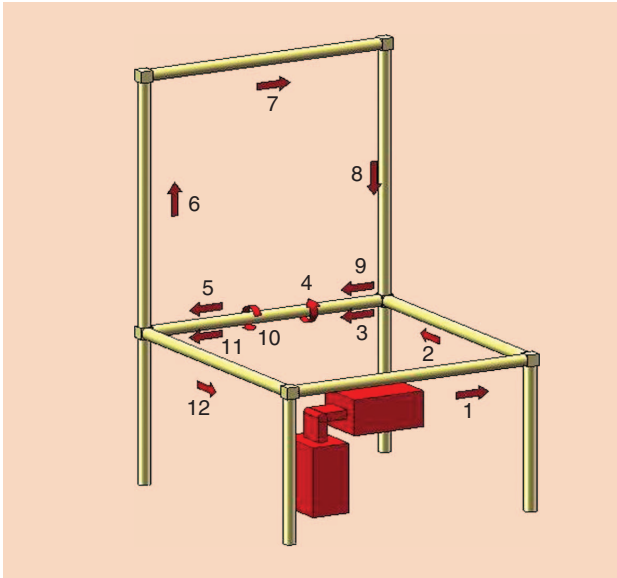


Figure 7. Robot motion in chairlike test structure.

Manipulation Motions (Robot R2)

R2 was designed to traverse a structure more robustly than R1 while adding the ability to manipulate the lockable truss connections. The robot demonstrated disassembly of a vertical square and disassembly and reassembly of a vertical and horizontal rod. These actions are shown in the demo video that accompanies this article.

Basic Motions

The three basic motions tested were translational motion, disassembly motion, and assembly motion. There are slight differences in the translational motions performed by robots R1 and R2 because of the use of stronger servos and the presence of sensors in robot R2.

1) *Translational Motion:* The robot starting position has both robot halves connected to rods with the translational mechanism engaged. The robot is attached below a horizontal rod. The robot could also be attached on top of the horizontal rod as an alternative starting point. The robot then performs the steps, as shown and described in Table 4.

The robot completes the motion with both translational mechanisms engaged at the center of the rod. The same steps would be performed, but in reverse order, to advance to the other end of the rod. Additionally, the same motion and steps could be performed on a vertical rod with the robot moving either up or down.

If the motion before or after the translational motion is a disassembly motion, the initial or final steps vary slightly. In the event that a disassembly just occurred, only one translational mechanism is engaged. If the robot moves to a rod with the intention to remove it, the robot will not engage the second translational mechanism but instead will start with the sequence to disassemble the rod.

2) *Disassembly Motion:* The disassembly motion starts with one-half of the robot connected to a horizontal rod via its

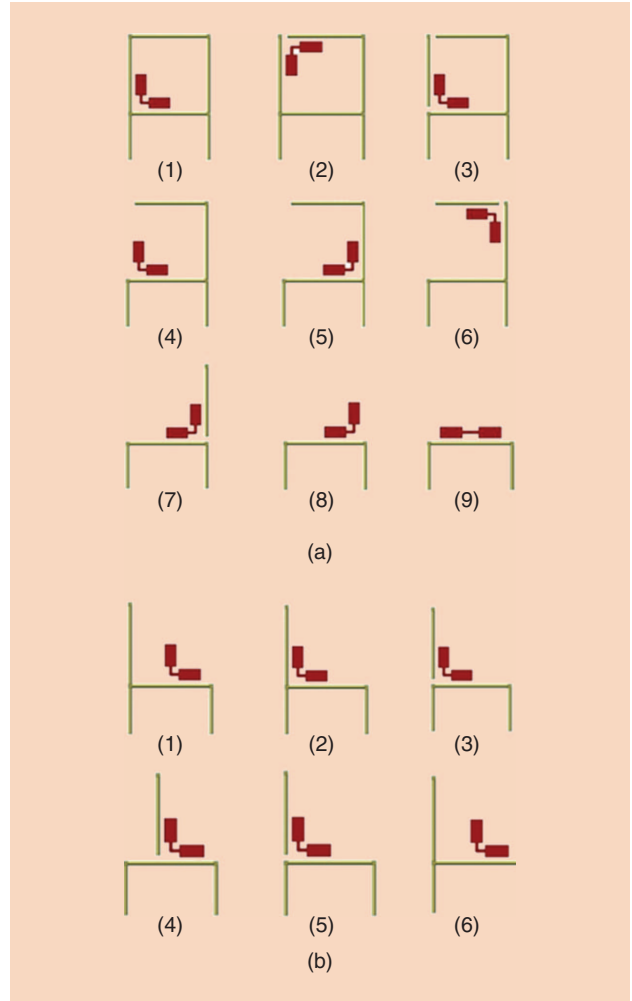


Figure 8. Disassembly and assembly motions: (a) vertical truss structure disassembly and (b) disassembly/assembly of vertical rod.

translational mechanism. The second half is at the rod to be disconnected. The robot then performs the steps as shown and described in Table 4.

When the rotational mechanism is engaged, feedback from the servos is used to gauge torque and rotation amount applied by the cam actuator. These readings are interpreted by the program to ensure proper rotational engagement has occurred. The robot will automatically realign, and re-engage itself until it has determined that the attachment will likely result in a successful disassembly.

- 3) *Assembly Motion:* For the assembly motion, the robot starts with one translational mechanism on one rod and the opposite rotational mechanism holding the rod to be connected to the node. The hinge is at an angle of 90°. The robot then performs the steps as shown and described in Table 4.
- 4) *Disassembly of a Horizontal Rod, 90° Rotation, and Assembly at a Different Point of the Connector:* This test was done to verify that a rod can be disconnected at one side of a connector and reconnected after a 90° rotation. This test was performed only once as a demonstration

that the system is robust enough to align itself correctly after the operation of the rotational mechanism. It is a starting point for allowing the robot to eventually reassemble an entire structure independently. For this motion, the robot is connected at the vertical rod with the translational mechanism engaged. The hinge is set at 90°. The robot then performs the steps as shown and described in Table 4.

Disassembly Test Bed—Vertical Square

The disassembly test bed is a vertical square plane in which the robot disassembles the top three rods of the structure. To disassemble the vertical structure, only a combination of the translational motions and the disassembly motions was necessary. The disassembly steps can be seen in Figure 8(a).

Assembly Test Bed—Single Truss

The assembly test bed consists of a single vertical rod. The rod was first unlocked and removed, then reattached and locked into place. The steps can be seen in Figure 8(b).

Results

We first examine the individual basic motions as described earlier and then display the overall results as obtained in the different test beds. The test beds are described in detail in the section “Test Bed.”

Robot R1 Traversal Test Results

- 1) *Basic Motions in Chairlike Test Structure:* The results of the chair traversal basic motion tests can be seen in Table 5. The overall success rates for the translational motion and the 90° vertical rotation were both above 90%. The success rate for the 180° horizontal rotation was only 42%. The average time for completion ranged from 11 to 14 s.
- 2) *Overall Test Results in Chairlike Test Structure:* Twelve tests were performed with two successful completions. This gave a success rate of 17% for the traversal of the complete structure. As can be surmised from the results of the basic movement tests, the majority of these failures on the chair structure were attributed to the incomplete 180° horizontal rotation. The other

errors were due to a broken structural part and a servo malfunction due to a program or servo error.

Robot R2 Assembly and Disassembly Test Results

- 1) *Basic Motions for Assembly and Disassembly Test:* The disassembly motions performed with robot R2 showed high success rates of 97% and 100% for the translational and disassembly motions, respectively. The assembly motion had a success rate of 70%.

- 2) *Overall Test Results for Assembly and Disassembly Tests:* Two different test beds were used for the assembly and disassembly tests. The assembly tests were demonstrated on a single vertical rod, as the robot currently does not possess a carrying mechanism. A total of 11 tests were conducted with seven successful completions of disassembly and reassembly. The rotational mechanism erroneously disengaged three times before the assembly was completed. One time the translational mechanism was disconnected from the horizontal rod during disassembly of the vertical rod.

Fourteen vertical square disassembly tests were performed, with ten of the 14 being completed successfully. Importantly, none of the failures were the result of design or programming flaws. The first failure was because of the battery running out of power. Therefore, tests 3–14 were performed with the power cable attached to the charging side of the battery (this had no impact on power delivered to the motors, as the supply voltage was regulated by the control board). Despite the battery being charged while performing the tests, another power failure was observed during test 12, likely the result of a loose power cable. During one of the tests, a rubber band had broken that was used to pull the mechanisms to the disengaged position. As for another test, the robot encountered an exception that resulted from the experimenter’s failure to remove a detached structural rod from the test structure.

Discussion

The tests showed that only three basic motions are needed for the robot to reach any point in the chairlike structure. Two out of the three basic motions needed to traverse in any structure were performed at high success rates of over 90%. The errors for the 90° vertical rotation were due to a broken

Table 5. Basic motions results.

	Movement in Chairlike Structure			Disassembly Tests		Assembly Tests
	Translational Motion	90° Vertical Rotation	180° Horizontal	Translational Motion	Disassembly Motion	Assembly Motion
Attempts	56	26	12	129	46	10
Successes	55	24	5	125	46	7
Success rate (%)	98	92	42	97	100	70
Time average (s)	12	14	11	18	11	6
Time standard deviation	0.9	0.5	1.2	3.2	0.9	0.4

structural part. This part is identical on robots R1 and R2, and during all the tests, this was the only time it broke; it could easily be designed to be stronger with no impact on the function of the robot and very little increase in weight.

The 180° horizontal rotation is the weakest of the basic motions required for movement in the structure. The errors were due to incomplete attachment of both rotational mechanisms. Fortunately, this is the least used motion, and both rotational motors were upgraded in R2 to alleviate this problem. Automatic engagement checking was also implemented to reduce these errors in R2. To complete a path as shown in Table 4, a combination of 16 translational motions, four 90° vertical rotation motions, and two 180° horizontal rotations are needed. The 180° horizontal rotation motion is not needed for disassembling a vertical plane. In R2, the reflectivity sensors could theoretically be used to assist in the verification of proper structural engagement, though this has not yet been implemented.

For structural disassembly and assembly, the robot had to be upgraded from R1 to R2, which included the addition of sensors for determining translational stopping points. The disassembly of a vertical structure was well performed by this robot because of the added accuracy lent by feedback from these sensors. The disassembly motion was performed with a 100% success rate, because the sensors could be used to reliably detect the ideal stopping point which ensured proper truss engagement. The translational motion success rate of R2 was comparable with the one obtained using robot R1. This shows that the use of stronger servos and line detection sensors in robot R2 compensated for the flexibility introduced by the lockable connectors.

The time to finish the translational motion was higher in R2, but this was only because of a decreased speed assigned in the programming.

The lockable connectors added a large amount of flexibility that resulted in a significant deflection from the vertical plane when the robot traversed up or down a single vertical rod. The 3-D printer cannot print the circular locking element accurately enough to ensure that tolerances are such that deflections are minimized. The deflection appears large but the connectors are strong enough to handle repeated abuse, as was demonstrated during the disassembly tests. The deflection angle can be seen in the demonstration video that accompanies this article.

R2 performed the assembly motion at a success rate of 70%. The errors observed are suspected to be the result of a communication error in the program. When the error is corrected, the success rate is expected to be above 90%, as was the case with the disassembly tests. Currently a design limitation is that the rods have to be assembled to the node from a specific direction.

The basic disassembly, 90° rotation, and reassembly of a horizontal rod were performed once for demonstration purposes. Its success confirms that the bidirectional gears and their self-centering ability are strong enough to reconnect a truss at new vertices of a connector element. This confirmation

opens up the possibility of creating a robot that can completely rebuild a structure.

The array of tests performed validate that the robot has the unique capability to disassemble any structure and provide limited reassembly options. As the current iteration of the robot is capable of reaching any point within the structure, complete disassembly is possible. Moreover, the rods that are needed for the construction of a structure, but not for the final design could be disassembled by the robot and reused. With the ability to traverse the structure in all directions and orientations, the robot could also be used to inspect a finished truss structure.

The biggest current hurdle for the robot is the absence of means for transporting rods across joints in the structure. This will be rectified in a future revision through the addition of a carrying pod. Difficulties will include maintaining a reasonable mass to power ratio and ensuring that the robot still has sufficient range of motion. Should the robot be implemented in a zero-gravity environment such as the international space station, attention to mass constraints would not be as critical.

Conclusion

In this article, we showed the design of a robot that can move autonomously and untethered through a truss structure. The robot demonstrated continuous motion over a total of eight nodes in a chairlike test structure and can successfully perform disassembly and assembly actions on a reconfigurable structure. These tests confirmed that the robot is capable of navigating through a vertical and a horizontal plane and transitioning between these planes because any cubic test structure consists of only vertical and horizontal planes and transitions between the planes. Only three basic motions were needed to move within the structure. Our novel adaptable connectors ensured that the robot could reliably disassemble and assemble horizontal and vertical trusses.

A combination of the motions demonstrated in this article theoretically allows the robot to take apart any size structure. For very large structures, the reliability of individual motions will need to be further improved; this can be accomplished by using our existing feedback system to allow the robot to assess itself more rigorously. A video motion tracking system, observing the structure, could also be employed to determine whether rods were removed or connected correctly and where errors occurred most commonly. This would be used only for gathering data; future versions of the robot will implement independent feedback, without the use of an external sensing system.

A carrying pod will eventually allow the robot to remove a rod from one location, carry it to another, and attach it there. Additionally, a mechanism for autonomously adding nodes will be implemented to facilitate an effective construction scheme. Disassembly and assembly with the ability to carry rods to any point in the structure and to add nodes open the door to reconfigurable and self-healing structures.

Future work will focus on improving reliability through increased sensor data, improved control schemes, and

superior error-correction actions. A carrying pod, a node-attachment mechanism, improved reliability, and motion error detection will allow us to create a robot and structure capable of nearly limitless configurations.

Acknowledgment

This work was supported in part by NSF EFRI Grant 0735953. The content of this paper is solely the responsibility of the authors and does not necessarily represent the official views of the sponsoring organization.

References

- [1] S. Skaff, P. Stariz, and W. L. Whittaker, "Skyworker: Robotics for space assembly, inspection and maintenance," in *Proc. Space Studies Inst. Conf.*, 2001, pp. 1–5.
- [2] S. Yun and D. Rus, "Self assembly of modular manipulators with active and passive modules," in *Proc. 2008 IEEE Int. Conf. Robotics Automation*, pp. 1477–1482.
- [3] W. Doggett, "Robotic assembly of truss structures for space systems and future research plans," in *Proc. 2002 IEEE Aerospace Conf.*, vol. 7, pp. 3589–3598.
- [4] K. C. Galloway, R. Jois, and M. Yim, "Factory floor: A robotically reconfigurable construction platform," in *Proc. 2010 IEEE Int. Conf. Robotics Automation*, pp. 2467–2472.
- [5] R. Aracil, R. J. Saltarén, and O. Reinoso, "A climbing parallel robot," *IEEE Robot. Autom. Mag.*, vol. 13, no. 1, pp. 16–22, Mar. 2006.
- [6] C. Balaguer, A. Gimenez, and M. Abderrahim, "ROMA robots for inspection of steel based infrastructures," *Ind. Robot: Int. J.*, vol. 29, no. 3, pp. 246–251, 2002.
- [7] P. Chatzakos, Y. P. Markopoulos, and K. Hrissagis, "On the development of a modular external-pipe crawling omni-directional mobile robot," *Ind. Robot: Int. J.*, vol. 33, no. 4, pp. 291–297, 2006.
- [8] I. M. Chen and S. H. Yeo, "Locomotion of a two-dimensional walking-climbing robot using a closed-loop mechanism: From gait generation to navigations," *Int. J. Robot. Res.*, vol. 22, no. 1, pp. 21–40, Jan. 2003.
- [9] K. A. Daltorio, T. E. Wei, A. D. Horchler, L. Southard, G. D. Wile, R. D. Quinn, S. N. Gorb, and R. E. Ritzmann, "Mini-Whegs climbs steep surfaces using insect-inspired attachment mechanisms," *Int. J. Robot. Res.*, vol. 28, no. 2, pp. 285–302, Feb. 2009.
- [10] M. Elliott, W. Morris, A. Calle, and J. Xiao, "City-climbers at work," in *Proc. 2007 IEEE Int. Conf. Robotics Automation*, pp. 2764–2765.
- [11] Y. Fu, Z. Li, and S. Wang, "A wheel-leg hybrid wall climbing robot with multi-surface locomotion ability," in *Proc. 2008 IEEE Int. Conf. Mechatronics Automation*, pp. 627–632.
- [12] G. J. Goldman, "Design space and motion development for a pole climbing serpentine robot featuring actuated universal joints," M.S. thesis, Dept. Mech. Eng., Virginia Polytech. Inst., Blacksburg, VA, 2009.
- [13] C. Hillenbrand, D. Schmidt, and K. Berns, "CROMSCI: Development of a climbing robot with negative pressure adhesion for inspections," *Ind. Robot: Int. J.*, vol. 35, no. 3, pp. 228–237, 2008.
- [14] L. P. Kalra, J. Gu, and M. Meng, "A wall climbing robot for oil tank inspection," in *Proc. IEEE Int. Conf. Robotics Biomimetics*, 2006, pp. 1523–1528.
- [15] B. Kennedy, A. Okon, H. Aghazarian, M. Badescu, X. Bao, Y. Bar-Cohen, Z. Chang, B. E. Dabiri, M. Garrett, L. Magnone, and S. Sherrit, "Lemur IIb: A robotic system for steep terrain access," *Ind. Robot: Int. J.*, vol. 33, no. 4, pp. 265–269, 2006.
- [16] K. D. Kotay and D. Rus, "Navigating 3-D steel web structures with an inchworm robot," in *Proc. 1996 IEEE/RSJ Int. Conf. Intelligent Robots Systems*, pp. 368–375.
- [17] S. P. Krosuri and M. A. Minor, "Design, modeling, control, and evaluation of a hybrid hip joint miniature climbing robot," *Int. J. Robots. Res.*, vol. 24, no. 12, pp. 1033–1053, Dec. 2005.
- [18] M. A. Minor and R. Mukherjee, "Under-actuated kinematic structures for miniature climbing robots," *J. Mech. Design*, vol. 125, no. 2, pp. 281–291, Jun. 2003.
- [19] T. P. Sattar, H. L. Rodriguez, and B. Bridge, "Climbing ring robot for inspection of offshore wind turbines," *Ind. Robot: Int. J.*, vol. 36, no. 4, pp. 326–330, 2009.
- [20] M. J. Spenko, G. C. Haynes, J. A. Saunders, M. R. Cutosky, and A. A. Rizzi, "Biologically inspired climbing with a hexapedal robot," *J. Field Robot.*, vol. 25, nos. 4–5, pp. 223–242, 2008.
- [21] D. Sun, J. Zhu, C. Lai, and S. K. Tso, "A visual sensing application to a climbing cleaning robot on the glass surface," *Mechatronics*, vol. 14, no. 10, pp. 1089–1104, 2004.
- [22] F. Tâche, W. Fischer, G. Caprari, R. Siegwart, R. Moser, and F. Mondada, "Magnebike: A magnetic wheeled robot with high mobility for inspecting complex-shaped structures," *J. Field Robot.*, vol. 26, no. 6, pp. 453–476, 2009.
- [23] M. Tavakoli, M. R. Zakerzadeh, G. R. Vossoughi, and S. Bagheri, "A hybrid pole climbing and manipulating robot with minimum DOFs for construction and service applications," *Ind. Robot: Int. J.*, vol. 32, no. 2, pp. 171–178, 2005.
- [24] M. Tavakoli, A. Marjovi, L. Marques, and A. T. de Almeida, "3DCLIMBER: A climbing robot for inspection of 3-D human made structures," in *Proc. 2008 IEEE/RSJ Int. Conf. Intelligent Robots Systems*, pp. 4130–4135.
- [25] T. S. White, R. Alexander, G. Callow, A. Cooke, S. Harris, and J. Sargent, "A mobile climbing robot for high precision manufacture and inspection of aerostructures," *Int. J. Robot. Res.*, vol. 24, no. 7, pp. 589–598, Jul. 2005.
- [26] Y. Yoon and D. Rus, "Shady3-D: A robot that climbs 3-D trusses," in *Proc. 2007 IEEE Int. Conf. Robotics Automation*, pp. 4071–4076.
- [27] D. A. Hjelle, "Toward machine metabolism: design of a truss reconfiguring robot," M.S. thesis, Sibley School Mech. Aerosp. Eng., Cornell Univ., Ithaca, NY, 2009.
- [28] C. Detweiler, M. Vona, Y. Yoon, S. Yun, and D. Rus, "Self-assembling mobile linkages," *IEEE Robot. Autom. Mag.*, vol. 14, no. 4, pp. 45–55, Dec. 2007.
- [29] Y. Terrada and S. Murata, "Automatic modular assembly system and its distributed control," *Int. J. Robot. Res.*, vol. 27, nos. 3–4, pp. 445–462, Mar./Apr. 2008.

Franz Nigl, Cornell Creative Machines Lab, Cornell University, Ithaca, NY 14853, USA. E-mail: franz.nigl@gmail.com

Shuguang Li, Northwestern Polytechnical University, Xi'an, Shaanxi 710072 and Cornell University, Ithaca, NY 14853, USA. E-mail: lisg81@gmail.com

Jeremy Evan Blum, Cornell Creative Machines Lab, Cornell University, Ithaca, NY 14853, USA. E-mail: jeb373@cornell.edu

Hod Lipson, Sibley School of Mechanical and Aerospace Engineering, Cornell University, Ithaca, NY 14853, USA. E-mail: hod.lipson@cornell.edu

